

Organic & Biomolecular Chemistry

Accepted Manuscript



This is an *Accepted Manuscript*, which has been through the Royal Society of Chemistry peer review process and has been accepted for publication.

Accepted Manuscripts are published online shortly after acceptance, before technical editing, formatting and proof reading. Using this free service, authors can make their results available to the community, in citable form, before we publish the edited article. We will replace this *Accepted Manuscript* with the edited and formatted *Advance Article* as soon as it is available.

You can find more information about *Accepted Manuscripts* in the [Information for Authors](#).

Please note that technical editing may introduce minor changes to the text and/or graphics, which may alter content. The journal's standard [Terms & Conditions](#) and the [Ethical guidelines](#) still apply. In no event shall the Royal Society of Chemistry be held responsible for any errors or omissions in this *Accepted Manuscript* or any consequences arising from the use of any information it contains.



Organic & Biomolecular Chemistry

ARTICLE

New PKS-NRPS tetramic acids and pyridinone from an Australian marine-derived fungus, *Chaunopycnis* sp.

Zhuo Shang,^a Li Li,^c Breno P. Espósito,^d Angela A. Salim,^a Zeinab G. Khalil,^a Michelle Quezada,^a Paul V. Bernhardt^b and Robert J. Capon^{a*}

Received 00th January 20xx,
Accepted 00th January 20xx

DOI: 10.1039/x0xx00000x

www.rsc.org/

Chemical analysis of a marine-derived fungus, *Chaunopycnis* sp. (CMB-MF028), isolated from the inner tissue of a pulmonate false limpet *Siphonaria* sp., collected from rock surfaces in the intertidal zone of Moora Park, Shorncliffe, Queensland, yielded the tetramic acid F-14329 (**1**) and new analogues, chaunolidines A–C (**2–4**), together with the new pyridinone chaunolidone A (**5**), and pyridoxatin (**6**). Structures inclusive of absolute configurations were assigned to **1–6** on the basis of detailed spectroscopic analysis, X-ray crystallography, electronic circular dichroism (ECD), biosynthetic considerations and chemical interconversion. Chaunolidine C (**4**) exhibits modest Gram-positive antibacterial activity (IC₅₀ 5–10 μM), while chaunolidone A (**5**) is a selective and potent inhibitor (IC₅₀ 0.09 μM) of human non-small cell lung carcinoma cells (NCI-H460). Tetramic acids **1–4** form metal chelates with Fe(III), Al(III), Cu(II), Mg(II) and Zn(II).

Introduction

In recent years, marine-derived fungi isolated from a range of substrates, including sediments, invertebrates, plants (mangroves) and algae, have been a prolific source of chemically diverse secondary metabolites. For example, our own investigations have yielded the anti-mycobacterial sydowiols¹ and brevianamides² from China Sea sediment isolates of *Aspergillus sydowii* and *Aspergillus versicolor*, as well as cyclopentapeptide cotteslosins,³ depsipeptide aspergillins⁴ and lipodepsipeptide acremolides⁵ from Australian beach-sand/estuarine isolates of *Aspergillus versicolor*, *Aspergillus carneus* and an *Acremonium* sp., respectively. In an effort to broaden our search, we recently isolated the fungus *Chaunopycnis* sp. (CMB-MF028) from inner tissue dissected from a pulmonate false limpet *Siphonaria* sp. collected near Moora Park, Shorncliffe, Queensland. Chemical fractionation of a broth cultivation of CMB-MF028 yielded the polyketide tetramic acid F-14329 (**1**) and three new analogues, chaunolidines A–C (**2–4**), as well as the new pyridinone chaunolidone A (**5**), and pyridoxatin (**6**). This report describes the production, isolation, characterization and structure elucidation of **1–**

6, including commentary on their biosynthesis and chemical interconversion, and spectroscopic and biological properties.

Results and discussion

The EtOAc extract from a broth cultivation of *Chaunopycnis* sp. (CMB-MF028) was concentrated *in vacuo* and the residue subjected to sequential solvent trituration (hexane, CH₂Cl₂ and MeOH). Reversed-phase fractionation of the CH₂Cl₂ and MeOH solubles yielded **1–6** (Figure 1).

HRESI(+)-MS analysis of **1** returned a pseudo-molecular ion indicative of a molecular formula (C₂₁H₂₇NO₅, Δ_{mmu} –0.1) requiring nine double bond equivalents (DBE), with the NMR (DMSO-*d*₆) data (Table 1) revealing resonances for two carbonyls, a *para*-disubstituted benzene, and four additional *sp*² carbons, with the remaining DBE attributed to a ring system (*i.e.* a tetramic acid). Diagnostic 2D NMR correlations (Figure 2) permitted identification of a polyketide subunit (C-1 to C-12) linked to a β-hydroxylated tyrosine (C-1' to C-9') via a tetramic acid moiety, with an *E* Δ^{8,9} configuration assigned by comparison of experimental and calculated ¹³C NMR chemical shifts for C-7 (δ_c 39.9) [*E*_{calc} δ_c 37.2; *Z*_{calc} δ_c 31.2] and C-10 (δ_c 17.8) [*E*_{calc} δ_c 17.6; *Z*_{calc} δ_c 11.6]. Of note, the NMR (CDCl₃) data for **1** revealed two equilibrating Δ^{2,3} geometric isomers (5:1) (ESI Figure S6 and Table S2), which on comparison with the ¹³C NMR data for *Z* and *E* isomers of the closely related tenuazonic acid (**7**)⁶ were attributed to major *Z* (δ_c 175.7, C-1; δ_c 194.7 C-1') and minor *E* (δ_c 169.2, C-1; δ_c 201.2, C-1') isomers of **1** (Figure 3). The *E/Z* equilibrium of the double bond between C-2/C-3 in CDCl₃ is a common characteristic for 3-acyltetramic acids (*e.g.* epicoccarine A,⁷ melophlins A and B,⁸ militarinones B and C,⁹ and vermelhotin¹⁰).

^a Institute for Molecular Bioscience, The University of Queensland, Brisbane, Queensland 4072, Australia. E-mail: r.capon@uq.edu.au; Fax: +61-7-3346-2090; Tel: +61-7-3346-2979

^b School of Chemistry and Molecular Biosciences, The University of Queensland, Brisbane, Queensland 4072, Australia

^c Beijing Key Laboratory of Active Substances Discovery and Druggability Evaluation, Institute of Materia Medica, Chinese Academy of Medical Sciences & Peking Union Medical College, Beijing 100050, China

^d Institute of Chemistry, University of São Paulo, 05508-000, São Paulo, Brazil
† Electronic Supplementary Information (ESI) available: general experimental procedures, NMR spectra and tabulated data for **1–6**, the lowest energy conformers of **1a** and **2a** for ECD calculation, HPLC profiles of the crude extract and dehydration/epimerization experiments, bioassays results, and fluorescence recovery curves after binding competition with iron. See DOI: 10.1039/x0xx00000x

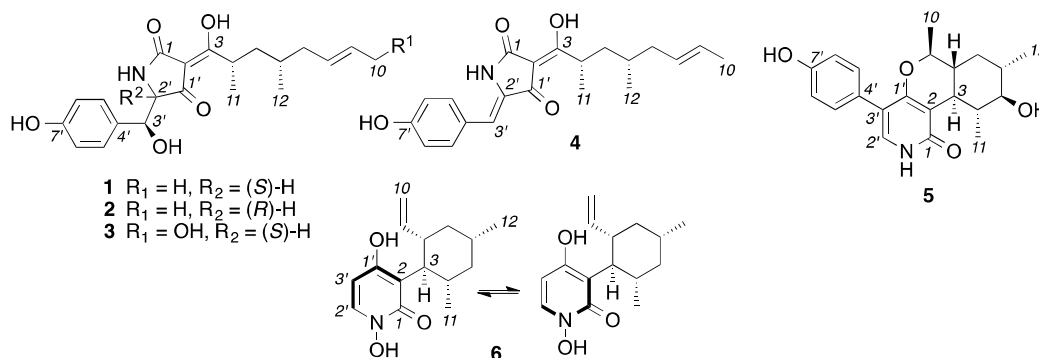


Fig. 1 PKS-NRPS metabolites 1–6 from *Chaunopycnis* sp. (CMB-MF028)

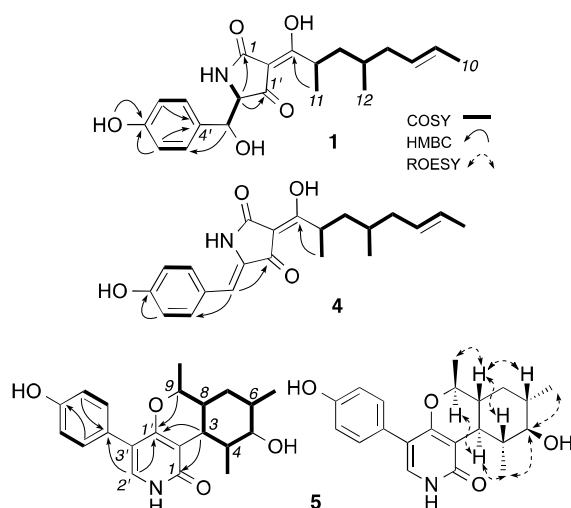


Fig. 2 Diagnostic 2D NMR (DMSO- d_6) correlations for 1, 4 and 5

Although only attributed a planar structure, the *Chaunopycnis* sp. metabolite F-14329, first patented in 2007 for its ability to lower murine postprandial blood triglyceride levels,¹¹ exhibited near identical NMR (ESI Table S4) and $[\alpha]_D$ data to **1**. More recently described in 2014 as one of a range of polyketides produced by epigenetic modifier challenged cultures of a *Tolypocladium* sp.,¹² the absolute and relative configuration for F-14329 (**1**) remain undetermined. Given the paucity of data in the primary literature and the absence of configurational assignments, we elected to unambiguously establish the absolute configuration of **1**, along with its co-metabolites **2–6** (see below).

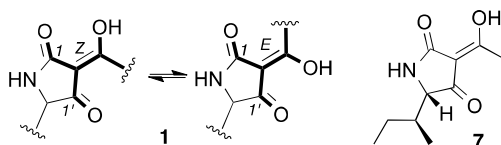


Fig. 3 NMR (CDCl₃) major (*Z*) and minor (*E*) $\Delta^{2,3}$ geometric isomers of **1**, and the structure for tenuazonic acid (**7**)

HRESI(+)^{MS} analysis established chaunolidine A (**2**) (C₂₁H₂₇NO₅, Δ_{mmu} +0.2) as an isomer of **1**, with analysis of the

NMR (DMSO- d_6) data (Table 1) disclosing the major difference as a deshielding of 11-H₃ ($\Delta\delta_{\text{H}}$ +0.2). Having discounted $\Delta^{2,3}$ geometric isomerism (see above), we hypothesized that **1** and **2** were diastereoisomers at C-2'. Consistent with this hypothesis, **1** and **2** were found to equilibrate via base-mediated (triethylamine or NaOH) C-2' epimerization (ESI Figure S17), a phenomena also reported for other tetramic acids (e.g. tenuazonic acid,¹³ harzianic acid¹⁴). Also supportive of this hypothesis, the staggered Newman projections about the C-2'–C-3' bond in **1** and **2** (Figure 4) demonstrated that C-2' epimerization induces significant differences in the relative proximity of 11-H₃ and the aromatic moiety.

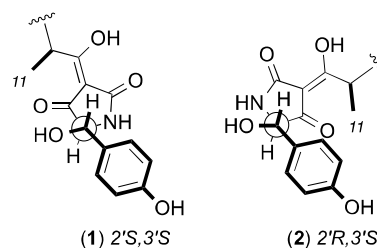
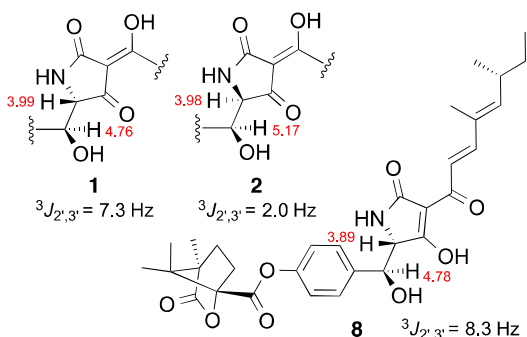
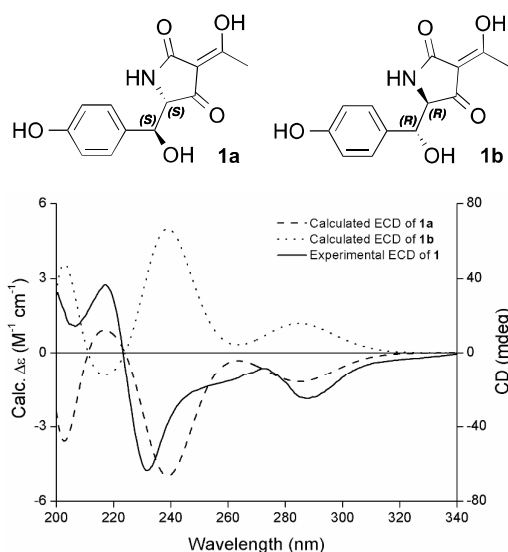


Fig. 4 Newman projections about C-2' to C-3' bond for **1** and **2**

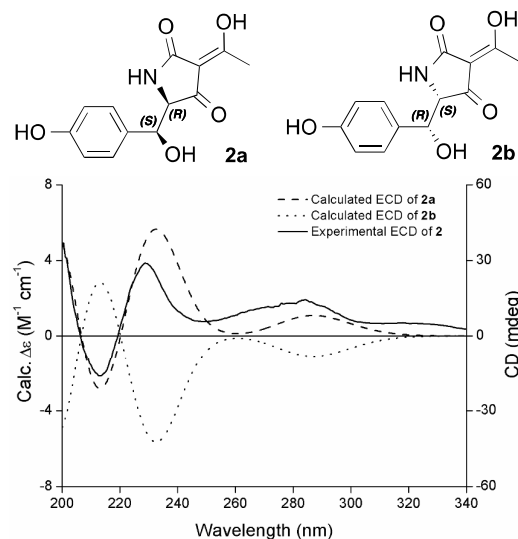
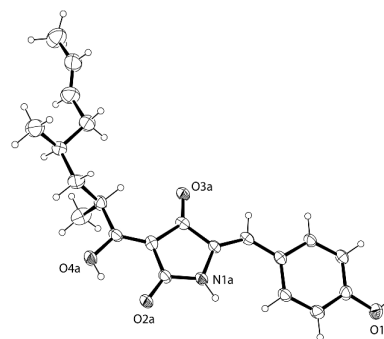
Attempts at preparing Mosher esters to independently confirm the C-3' absolute configuration proved unsuccessful, as both **1** and **2** undergoing facile dehydration to yield chaunolidine C (**4**) (see below). Nevertheless, comparison of the ¹H NMR chemical shifts and ³J coupling constants (in CDCl₃) of 2'-H/3'-H in **1** and **2** with that of prototenellin D camphanyl ester (**8**), where the absolute configuration had been previously determined by X-ray analysis (2'S,3'S),¹⁵ suggested that **1** possessed a 2'S,3'S or 2'R,3'R configuration, while **2** was either 2'R,3'S or 2'S,3'R (Figure 5). In our hands the absolute configurations for **1** (2'S,3'S) and **2** (2'R,3'S) were determined by comparison of experimental and predicted ECD (time-dependent density functional theory, B3LYP/6-31g(d)) spectra for the model compounds **1a,b** and **2a,b**, respectively (Figures 6 and 7). Although tetramic acids comprising similar functionality to **1** and **2** have been reported in recent years (e.g. militarinones,⁹ prototenellins¹⁵ and epicoccarines¹⁶), to the best of our knowledge, this is the first occasion where absolute configurations have been determined without recourse to total synthesis or X-ray analysis of the synthetic derivatives.

Fig. 5 Comparison of δ_{H} and ${}^3J_{2,3'}$ between **1**, **2** and **8**Fig. 6 The experimental ECD (MeOH) spectra for **1** and the calculated spectra for **1a** and **1b**

HRESI(+)-MS analysis of **3** revealed a molecular formula ($\text{C}_{21}\text{H}_{27}\text{NO}_6$, $\Delta\text{mmu} -0.2$) suggestive of a hydroxylated analogue of **1**. Comparison of 1D and 2D NMR ($\text{DMSO}-d_6$) data for **3** and **1** supported this hypothesis, with the only significant difference being oxidation of the allylic primary methyl in **1** (C-10, δ_{H} 1.59, δ_{C} 17.8) to an allylic primary alcohol in **3** (C-10, δ_{H} 3.85, δ_{C} 61.4). These NMR comparisons, together with comparable Cotton effects [λ_{max} ($\Delta\epsilon$), 235 (−11.4), 288 (−6.4)], suggested that **1** and **3** share a common 2'S,3'S configuration, and that the structure for chaunolidine B (**3**) (less configurations about C-4 and C-6) be assigned as indicated (Figure 1).

HRESI(−)-MS analysis of **4** returned a molecular formula ($\text{C}_{21}\text{H}_{25}\text{NO}_4$, $\Delta\text{mmu} -0.1$) indicative of a dehydration analogue of **1**. Comparison of the 1D NMR ($\text{DMSO}-d_6$) data for **4** with **1** confirmed the loss of resonances for 2'-H and 3'-H sp^3 methines, and the appearance of resonances for a 3'-H sp^2 methine (δ_{H} 6.45) embedded in a trisubstituted $\Delta^{2,3'}$, while diagnostic 2D NMR correlations (Figure 2) permitted assignment of the planar structure. A single crystal X-ray diffraction analysis of **4** (as its methanol solvate) (Figure 8) permitted unambiguous assignment of the absolute structure for chaunolidine C (**4**) as indicated (Figure 1), including $\Delta^{2,3'}$ Z, 4S and 6S configurations. With two molecules of **4** (and

MeOH) in the asymmetric unit possessing essentially the same conformation, the absolute configuration of **4** was established from a statistical analysis of anomalous dispersion effects of 2938 Bijvoet pairs using the method of Hooft *et al.*¹⁷ leading to a probability (P_2) of the correct enantiomer being 0.99 (Hooft parameter 0.1(3), $\nu = 15$ using Student's *t*-statistics). As both **1** and **2** experienced acid-mediated (TFA or HCl) dehydration and conversion to **4** (ESI Figure S18), **1–2** and **4** were assigned a common 4S,6S configuration, which on biosynthetic grounds was extended to **3**. Thus the structures with complete configurations for F-14329 (**1**) and chaunolidines A–C (**2–4**) are assigned as indicated in Figure 1.

Fig. 7 The experimental ECD (MeOH) spectra for **2** and the calculated spectra for **2a** and **2b**Fig. 8 ORTEP³⁴ structure generated from the single crystal X-ray diffraction of **4** showing 30% probability ellipsoids

Finally, to establish that **2** and **4** were natural products (not mere handling artefacts), a neutral pH HPLC-DAD-MS analysis confirmed both were present in the EtOAc extract of a fresh recultivation of CMB-MF028 (ESI Figure S1).

HRESI(+)-MS analysis of **5** returned a molecular formula ($\text{C}_{21}\text{H}_{25}\text{NO}_4$) isomeric with **4**, with NMR ($\text{DMSO}-d_6$) data (Table 2) revealing resonances for one carbonyl, a *para*-substituted benzene, and four sp^2 carbons, necessitating a tetracyclic structure. Diagnostic HMBC and COSY 2D NMR correlations supported this conclusion, and permitted assembly of the planar structure for **5** (Figure 2), while

Table 1. NMR (600 MHz, DMSO-*d*₆) data for F-14329 (1) and chaunolidines A–C (2–4)

Pos.	1		2		3		4	
	δ_{H} (mult., <i>J</i> (Hz))	δ_{C}						
1	–	176.0	–	176.4	–	176.0	–	– ^F
2	–	100.6	–	101.1	–	100.5	–	– ^F
3	–	191.5	–	190.6	–	191.5	–	199.2 ^E
4	3.49 (m)	33.4	3.63 ^D	33.2	3.48 (br s)	33.3	3.82 (m)	35.9 ^E
5a	1.62 (m) ^B	39.8 ^D	1.68 (m)	39.8 ^D	1.62 (m)	39.4 ^D	1.75 (m) ^A	39.8 ^D
5b	1.04 (m)	–	1.11 (m) ^A	–	1.06 (m)	–	1.14 (m) ^B	–
6	1.24 (m)	30.8	1.29 (m)	30.7	1.28 (m)	30.7	1.36 (m)	30.8
7a	1.86 (m)	39.9 ^D	1.91 (m)	39.9 ^D	1.92 (m)	39.7 ^D	1.94 (m)	39.9 ^D
7b	1.74 (m)	–	1.77 (m)	–	1.77 (m)	–	1.78 (m) ^A	–
8	5.33 (m) ^A	129.3 ^C	5.36 (m) ^B	129.4	5.48 (m) ^A	132.1	5.36 (m) ^C	129.4
9	5.34 (m) ^A	125.9	5.38 (m) ^B	125.9	5.47 (m) ^A	127.9	5.37 (m) ^C	125.9
10	1.59 (d, 5.2) ^B	17.8	1.62 (d, 5.0)	17.8	3.85 (br s)	61.4	1.60 (d, 4.2)	17.8
11	0.88 (d, 6.3)	18.1	1.08 (d, 6.7) ^A	18.1	0.88 (d, 6.5)	18.1	1.12 (d, 6.2) ^B	18.0
12	0.77 (d, 6.3)	19.1	0.80 (d, 6.6)	19.3	0.78 (d, 6.2)	19.1	0.83 (d, 6.6)	19.3
1'	–	192.6	–	193.4	–	192.6	–	181.1 ^E
2'	4.16 (br s)	68.0	3.95 (br s)	67.8	4.16 (br s)	68.0	–	– ^F
3'	4.87 (br d, 3.1)	72.6	4.82 (br s)	71.1	4.87 (br s)	72.6	6.45 (s)	110.2 ^E
4'	–	129.3 ^C	–	132.1	–	129.3	–	123.9
5'/9'	7.00 (d, 8.5)	128.2	7.14 (d, 8.4)	127.3	7.00 (d, 8.2)	128.2	7.52 (d, 8.6)	131.8
6'/8'	6.59 (d, 8.5)	114.1	6.69 (d, 8.4)	114.7	6.59 (d, 8.2)	114.1	6.79 (d, 8.6)	115.8
7'	–	156.5	–	156.5	–	156.5	–	158.3
3'-OH	5.65 (br s)	–	5.41 (br s) ^B	–	5.64 (br s)	–	–	–
7'-OH	9.23 (br s)	–	9.26 (s)	–	9.23 (s)	–	9.92 (br s)	–
-NH	9.14 (br s)	–	8.59 (br s)	–	9.15 (br s)	–	–	–

^{A–C} Assignments with the same superscript within a column are overlapping signals and can be interchangeable. ^D Overlap with residual DMSO or H₂O signals. ^E Assignments supported by HSQC and HMBC. ^F Carbon signals are weak or broad that cannot be seen in ¹³C NMR spectrum

ROESY correlations positioned 3-H, 11-H₃ and 12-H₃ on one (α) face, and 4-H, 8-H and 10-H₃ on the opposite (β) face of the cyclohexanyl ring. On biosynthetic grounds we propose that **5** possesses the same configuration about C-4 and C-6 as the co-metabolites **1–4**, permitting assignment of the structure for chaunolidone A (**5**) as indicated (Figure 1).

The major *Chaunopycnis* sp. (CMB-MF028) metabolite was identified on the basis of detailed spectroscopic analysis as pyridoxatin (**6**) (Figure 1). First reported in 1991 as an equilibrating mixture of atropisomers from the fungus *Acremonium* sp. (BX86),¹⁸ the absolute configuration of **6** was only assigned in 2014 by X-ray diffraction analysis of the metal chelate, (pyridoxatin)₂Cu.¹²

The biosynthesis of tetramic acids and pyridinones has been extensively studied,^{16,19} indicating a common PKS-NRPS origin in which a tyrosine substrate undergoes successive thioester condensations inclusive of reductive cleavage, ring closure and oxidation, to yield the epimeric tetramic acids **1** and **2**. Further oxidation of the aliphatic side chain in **1** can lead to **3**, while dehydration delivers **4**. Oxidative ring expansion links the tetramic acid and pyridinone scaffolds, with side chain cyclization and hydroxylation returning **5**. It is noteworthy that **6** can be formed by phenol cleavage after cyclization of the side chain, as recently documented by stable isotope labelling studies.¹²

Numerous natural products containing the tetramic acid scaffold isolated from diverse biological sources (e.g. plants, sponges, bacteria and fungi), display a wide array of biological activities

including antibacterial,^{20,21} antifungal,²² antiviral²³ antitumor,^{8,24} anti-inflammatory²⁵ and herbicidal activities,²⁶ as well as metal ion chelating properties.^{24,27} To explore their biological potential we screened the co-metabolites **1–6** in antibiotic, cytotoxicity and metal ion chelating assays.

The antibiotic properties of **1–6** were evaluated against Gram-positive bacteria *Staphylococcus aureus* (ATCC 25923), *Staphylococcus epidermidis* (ATCC 12228) and *Bacillus subtilis* (ATCC 6633), Gram-negative bacteria *Escherichia coli* (ATCC 25922), *Pseudomonas aeruginosa* (ATCC 27853) and *Klebsiella pneumoniae* (ATCC 13883), and a fungus *Candida albicans* (ATCC 90028). Only chaunolidine C (**4**) exhibited antibacterial activity, with modest levels of growth inhibition against all three aerobic Gram-positive bacteria (IC₅₀ 5–10 μ M) (ESI Table S11, Figure S19).

The cytotoxic properties of **1–6** were evaluated in growth inhibition assays against human colorectal adenocarcinoma (SW620), non-small cell lung carcinoma (NCI-H460) and cervical carcinoma (KB3-1) cells. While none of the tetramic acids **1–4** exhibited cytotoxic activity, chaunolidone A (**5**) was a selective and potent cytotoxin to NCI-H460 cells (IC₅₀ 0.09 μ M) (ESI Table S12, Figure S20). Consistent with literature accounts,²⁸ pyridoxatin (**6**) exhibited potent but non-selective cytotoxicity against all three human cancer cell lines (IC₅₀ 0.3–0.4 μ M).

Table 2. NMR (600 MHz, DMSO-*d*₆) data for chaunolidone A (5)

Pos.	δ_{H} (mult., <i>J</i> (Hz))	δ_{C}
1	–	162.6
2	–	111.6
3	2.62 (dd, 10.5, 10.3)	36.1
4	1.72 (m)	44.3
5	3.38 ^C	74.7
6	1.60 (m)	37.2
7 α	1.16 (m) ^B	30.6
7 β	1.40 (m) ^A	–
8	1.37 (m) ^A	48.9
9	3.66 (m)	77.7
10	1.19 (d, 6.2) ^B	18.9
11	1.10 (d, 6.9)	19.5
12	0.93 (d, 6.7)	18.6
1'	–	162.5
2'	6.99 (s)	130.1
3'	–	113.1
4'	–	125.1
5'/9'	7.17 (d, 8.5)	129.9
6'/8'	6.72 (d, 8.5)	114.8
7'	–	156.2
7'-OH	10.93 (br s)	–
-NH	9.37 (br s)	–

^{A,B} Overlapping signals. ^C Overlap with residual H₂O signals.

Although the ecological roles of **1–6** are not known, tetramic acid (e.g. **1–4**) and pyridinone (e.g. **5–6**) moieties feature prominently in many siderophores. Siderophores are crucial to the survival of many microbes, facilitating the uptake of iron and other trace metals from the surrounding environment. Importantly, siderophores are especially significant in the marine environment where metal ion concentrations typically fall below 10⁻⁶ M.²⁹ To assess the metal chelation capacity of **1–6** we employed a calcein-Fe(III) complex (CAFe) assay.

Calcein is a fluorescent chelator with high affinity for Fe(III). As metal coordination with calcein leads to stoichiometric fluorescence quenching, this effect can be employed to quantify labile iron concentrations in biological media.³⁰ Similarly, a competing equilibrium between candidate iron chelators, and the complex calcein-Fe(III) (CAFe), can be used to assess the relative affinity of putative chelators for Fe(III). In our study, analytes **1–6** were assessed for their ability to bind Fe(III), disrupting the CAFe complex and releasing fluorescent calcein which was quantified fluorometrically. In the CAFe assay, only pyridoxatin (**6**) exhibited a strong affinity for Fe(III) with an apparent stability constant ($\log K_{\text{app}}$) of 34 assuming the binding stoichiometry of **6** and Fe(III) is 3:1, and with K_{app} derived from physiological buffer. Although not directly comparable, this value for **6** is within the same magnitude as stability constants ($\log \beta$) determined for other chelators such as desferrioxamine ($\log \beta = 31$)³¹ or deferiprone ($\log \beta = 35$).³² Notwithstanding the inability of **1–5** to extract Fe(III) from CAFe, treatment of **1–5** with various metal salts in MeOH did permit the ready HRESI(±)MS detection of Fe(III), Al(III), Cu(II), Mg(II) and

Zn(II) metal complexes of **1–4** (ESI Table S13), suggesting that **1–4** were modest but non-selective metal ion chelators.

Experimental

Fungal strain collection

The fungus *Chaunopycnis* sp. (CMB-MF028) was isolated from the inner tissue of a marine pulmonate false limpet *Siphonaria* sp. collected in 2012 from rock surfaces in the intertidal zone of Moora Park, Shorncliffe, Queensland. Freshly collected *Siphonaria* specimens were transported to the laboratory at 0 °C in sealed Falcon tubes (50 mL), after which they were rinsed in sterile seawater, and their external surfaces were disinfected by submersion in 70% EtOH/H₂O for 30 s. After surface sterilization, the *Siphonaria* samples were washed with sterile seawater and subjected to aseptic dissection. Small pieces of inner tissue were applied to PYG agar plates (comprising 2% glucose, 1% peptone, 0.5% yeast extract, 0.02% chloramphenicol and 1.5% agar in 50% artificial seawater) and the plates sealed with parafilm and incubated for 3–4 weeks. A pure culture of CMB-MF028, obtained by single-colony serial transfer on agar plates was cryopreserved at –80 °C in 15% aqueous glycerol.

Analytical cultivation and chemical profiling

Chaunopycnis sp. (CMB-MF028) was cultivated at 200 rpm for 9 d in a Schott flask (250 mL) containing ISP-2 broth (0.4% glucose, 0.4% yeast extract and 1% malt extract in 80 mL distilled water). After cultivation, the broth was extracted with EtOAc (60 mL) and the organic phase concentrated *in vacuo* to yield a crude extract (9.5 mg). A solution of crude extract prepared in MeOH (5 mg/mL) was subjected to HPLC-DAD-ESI(±)MS analysis (Zorbax SB-C₈ column, 150 × 4.6 mm column, 5 μ m, 1 mL/min gradient elution from 90% H₂O/MeCN to 100% MeCN over 15 min, with constant 0.05% formic acid modifier).

Production, isolation and characterization of **1–6**

A seed culture of *Chaunopycnis* sp. (CMB-MF028) was prepared by inoculating a Schott flask (250 mL) containing PYG broth (50 mL, comprising 2% glucose, 1% peptone and 0.5% yeast extract in 50% artificial seawater) with mycelia from an agar plate cultivation, and incubating at 200 rpm at 26.5 °C for 3 d. Six 2 L Erlenmeyer flasks containing ISP-2 broth (500 mL) inoculated with seed culture (5 mL) were incubated at 200 rpm at 26.5 °C for 9 d, after which the consolidated broth was extracted with EtOAc (3 × 3 L) and the combined organic phase was concentrated *in vacuo* at 40 °C to afford the crude extract (681.5 mg). The crude extract was then sequentially triturated to yield hexane (34.8 mg), CH₂Cl₂ (297.0 mg) and MeOH (215.2 mg) soluble material.

The CH₂Cl₂ solubles were subjected to SPE fractionation (GracePure C₁₈ Max, 10% stepwise gradient elution from 90% H₂O/MeOH to 100% MeOH) to yield Fractions C1–10. Fractions C6 and C7 were combined (65.3 mg) and subjected to HPLC fractionation (Zorbax SB-C₈ column, 250 × 9.4 mm, 5 μ m, 3 mL/min gradient elution from 45% to 35% H₂O/MeCN over 15 min, with constant 0.01% TFA modifier) to yield F-14329 (**1**) ($t_{\text{R}} = 8.83$ min; 9.6 mg, 1.41%) and chaunolidone A (**2**) ($t_{\text{R}} = 9.85$ min; 1.3 mg, 0.19%). Fraction C4 (20.4 mg) was subjected to HPLC fractionation

(Zorbax SB-C₈ column, 250 × 9.4 mm, 5 μm, 3 mL/min gradient elution from 70% to 60% H₂O/MeCN over 15 min, with constant 0.01% TFA modifier) to yield chaunolidine B (**3**) (*t_R* = 11.07 min; 2.6 mg, 0.38%). Fraction C8 (18.8 mg) was subjected to HPLC fractionation (Zorbax SB-C₈ column, 250 × 9.4 mm, 5 μm, 3 mL/min gradient elution from 25% to 15% H₂O/MeCN over 15 min, with constant 0.01% TFA modifier) to yield chaunolidine C (**4**) (*t_R* = 7.42 min; 4.7 mg, 0.69%).

The MeOH solubles were subjected to SPE fractionation (GracePure C₁₈ Max, 10% stepwise gradient elution from 90% H₂O/MeOH to 100% MeOH) to yield Fractions M1-10. Fraction M6 (69.6 mg) was subjected to HPLC fractionation (Zorbax SB-C₈ column, 250 × 9.4 mm, 5 μm, 3 mL/min gradient elution from 55% to 35% H₂O/MeCN over 15 min, with constant 0.01% TFA modifier) to yield chaunolidone A (**5**) (*t_R* = 9.17 min; 4.2 mg, 0.62%). Fractions M7 and M8 were combined (72.7 mg) and were subjected to HPLC fractionation (Zorbax SB-C₈ column, 250 × 9.4 mm, 5 μm, 3 mL/min gradient elution from 45% to 30% H₂O/MeCN over 15 min, with constant 0.01% TFA modifier) to yield pyridoxatin (**6**) (*t_R* = 7.13 min; 22.6 mg, 3.32%).

Note: % yields for compounds **1–6** are calculated as weight-to-weight estimate against the crude extract.

F-14329 (1). Colourless oil; $[\alpha]_D^{22}$ -216.9 (*c* 0.05, MeOH); UV-vis (MeCN) λ_{\max} (log ϵ) 225 (4.12), 279 (4.20) nm; CD (MeOH) λ_{\max} ($\Delta\epsilon$) 217 (+10.4), 232 (-18.0), 273 (-2.4), 288 (-7.1) nm; NMR (600 MHz, DMSO-*d*₆) see Table 1 and ESI Table S1; ESI(+)-MS *m/z* 396 [M + Na]⁺, 356 [M - H₂O + H]⁺, ESI(-)-MS *m/z* 372 [M - H]⁻; HRESI(+)-MS *m/z* 396.1782 [M + Na]⁺ (calcd for C₂₁H₂₇NO₅Na⁺, 396.1781).

Chaunolidine A (2). Colourless oil; $[\alpha]_D^{22}$ +70.4 (*c* 0.05, MeOH); UV-vis (MeCN) λ_{\max} (log ϵ) 225 (4.06), 279 (4.18) nm; CD (MeOH) λ_{\max} ($\Delta\epsilon$) 213 (-3.7), 229 (+6.5), 249 (+1.3), 284 (+3.3) nm; NMR (600 MHz, DMSO-*d*₆) see Table 1 and ESI Table S5; ESI(+)-MS *m/z* 396 [M + Na]⁺, 356 [M - H₂O + H]⁺, ESI(-)-MS *m/z* 372 [M - H]⁻; HRESI(+)-MS *m/z* 396.1779 [M + Na]⁺ (calcd for C₂₁H₂₇NO₅Na⁺, 396.1781).

Chaunolidine B (3). Colourless oil; $[\alpha]_D^{22}$ -147.7 (*c* 0.05, MeOH); UV-vis (MeCN) λ_{\max} (log ϵ) 225 (4.11), 279 (4.16) nm; CD (MeOH) λ_{\max} ($\Delta\epsilon$) 208 (+4.9), 218 (+8.3), 235 (-11.4), 272 (+1.5), 288 (-6.4) nm; NMR (600 MHz, DMSO-*d*₆) see Table 1 and ESI Table S7; ESI(+)-MS *m/z* 372 [M - H₂O + H]⁺, 354 [M - 2H₂O + H]⁺, ESI(-)-MS *m/z* 388 [M - H]⁻; HRESI(+)-MS *m/z* 412.1733 [M + Na]⁺ (calcd for C₂₁H₂₇NO₆Na⁺, 412.1731).

Chaunolidine C (4). Yellow solid; $[\alpha]_D^{22}$ -73.3 (*c* 0.05, MeOH); UV-vis (MeOH) λ_{\max} (log ϵ) 267 (4.26), 338 (4.47) nm; NMR (600 MHz, DMSO-*d*₆) see Table 1 and ESI Table S8; ESI(+)-MS *m/z* 356 [M + H]⁺, 378 [M + Na]⁺, ESI(-)-MS *m/z* 354 [M - H]⁻; HRESI(-)-MS *m/z* 354.1712 [M - H]⁻ (calcd for C₂₁H₂₄NO₄⁻, 354.1711).

Chaunolidone A (5). Colourless oil; $[\alpha]_D^{22}$ -81.3 (*c* 0.05, MeOH); UV-vis (MeCN) λ_{\max} (log ϵ) 212 (4.23), 250 (4.19) nm; NMR (600 MHz, DMSO-*d*₆) see Table 2 and ESI Table S9; ESI(+)-MS *m/z* 356 [M + H]⁺, ESI(-)-MS *m/z* 354 [M - H]⁻; HRESI(+)-MS *m/z* 378.1676 [M + Na]⁺ (calcd for C₂₁H₂₅NO₄Na⁺, 378.1676).

Pyridoxatin (6). Off-white crystal; $[\alpha]_D^{22}$ -34.0 (*c* 0.05, MeOH); UV-vis (MeCN) λ_{\max} (log ϵ) 215 (4.52), 293 (3.91) nm; CD (MeOH) λ_{\max} ($\Delta\epsilon$) 207.5 (-11.6), 285.5 (+1.0) nm; NMR (600 MHz, DMSO-*d*₆) see ESI Table S10; ESI(+)-MS *m/z* 264 [M + H]⁺, 286 [M + Na]⁺, ESI(-)-MS *m/z* 262 [M - H]⁻; HRESI(+)-MS *m/z* 286.1414 [M + Na]⁺ (calcd for C₁₅H₂₁NO₃Na⁺, 286.1414).

Base-mediated equilibration of **1** and **2**

Samples of **1** (20 μg) and **2** (20 μg) were treated at r.t. for 12 h with either (i) 50% triethylamine (TEA) in MeOH (50 μL) or (ii) 0.01 M NaOH in MeOH (50 μL), after which the reaction mixture was concentrated to dryness under dry N₂, and redissolved in MeOH (50 μL) prior to HPLC-DAD-ESI(±)MS analysis (Zorbax SB-C₈ column, 150 × 4.6 mm column, 5 μm, 1 mL/min gradient elution from 90% H₂O/MeCN to 100% MeCN over 15 min, with constant 0.05% formic acid modifier). These analyses (ESI Figure S17) demonstrate that **1** and **2** undergo base-mediated equilibration.

Acid-mediated dehydration of **1** and **2**

Samples of **1** (20 μg) and **2** (20 μg) were treated at r.t. for 12 h with either (i) 50% trifluoroacetic acid (TFA) in MeOH (50 μL) or (ii) 0.01 M HCl in MeOH (50 μL), after which the reaction mixture was concentrated to dryness under dry N₂, and redissolved in MeOH (50 μL) prior to HPLC-DAD-ESI(±)MS analysis (Zorbax SB-C₈ column, 150 × 4.6 mm column, 5 μm, 1 mL/min gradient elution from 90% H₂O/MeCN to 100% MeCN over 15 min, with constant 0.05% formic acid modifier). These analyses (ESI Figure S18) demonstrate that **1** and **2** undergo acid-mediated dehydration to yield **4**.

ECD calculation of **1** and **2**

Given that two methyl groups on the side chain have negligible contribution to ECD spectra (proved by ECD calculation in pre-experiment), two pairs of enantiomers (**1a** and **1b**; **2a** and **2b**) were used as model compounds of **1** and **2** by replacing the flexible side chain at C-4 with a methyl group to simplify the calculation. Conformation analyses of **1a** and **2a** were performed using the MMFF94 molecular mechanics force field via the Molecular Operating Environment (MOE) software package (Chemical Computing Group, Canada). Within the energy of 6 kcal/mol, **1a** showed four lowest energy conformers with distribution of 97.31%, 2.48%, 0.17% and 0.04% (ESI Figure S2), and **2a** also has four lowest energy conformers with distribution of 53.93%, 41.08%, 4.37% and 0.62% (ESI Figure S3). These conformers were subsequently optimized with Gaussian09 software package at the B3LYP/6-31g(d) level using density-functional theory (DFT) method. Conformation analysis and frequency calculation demonstrated that these conformers are all stable in methanol. The 40 lowest electronic transitions for each stable conformer were calculated using time-dependent density functional theory (TDDFT) method at the B3LYP/6-31g(d) level. ECD spectrum of each conformer was then simulated using a Gaussian function with a half-bandwidth of 0.25 eV. The overall calculated ECD spectra of **1a** and **2a** were generated on the basis of Boltzman weighting of individual conformers.

X-ray crystallographic analysis of 4•MeOH

The single crystal of 4•MeOH was obtained from MeOH by slow evaporation at r.t. Data were collected at 190 K using an Oxford Diffraction Gemini CCD diffractometer with Cu K α radiation and the crystal was cooled with an Oxford Cryosystems Desktop Cooler. Data reduction was performed with the CrysAllisPro program (Oxford Diffraction vers. 171.34.40). The structure was solved by direct methods with SHELXS86 and refined with SHELXL97.³³ The thermal ellipsoid diagram was produced with ORTEP³⁴ and all calculations were performed within the WinGX package.³⁵

Crystal data of 4•MeOH C₂₁H₂₅NO₄•CH₃OH, *M* = 387.46, triclinic, *a* = 6.6012(4), *b* = 8.1654(6), *c* = 19.831(1) Å, *V* = 1056.7(1) Å³, *T* = 190(2) K, space group *P*1, *Z* = 2, 13470 reflections measured, 6294 unique (*R*_{int} = 0.0506) which were used in all calculations. The final *R*(obs. data) was 0.0658, goodness of fit 1.031. CCDC number 1402566.

Conclusions

In summary, four tetramic acids (1–4) and two pyridinone derivatives (5–6) were purified and identified from a marine gastropod mollusc *Siphonaria* sp. associated fungus *Chaunopycnis* sp. (CMB-MF028). Structures inclusive of absolute configurations were established by detailed spectroscopic analysis, ECD spectra, X-ray crystallography, chemical conversion and biosynthetic considerations. Chaunolidine C (4) exhibited modest Gram-positive antibacterial activity (IC₅₀ 5–10 μM), while chaunolidone A (5) displayed potent and selective cytotoxicity towards human non-small cell lung carcinoma cells (IC₅₀ 0.09 μM). F-14329 (1) and chaunolidines A–C (2–4) are weak and non-selective metal chelators, while pyridoxatin (6) is a potent and selective siderophore with a high affinity to Fe(III) (log*K*_{app} = 34).

Acknowledgements

The authors gratefully acknowledge R. H. Cichewicz (University of Oklahoma) for providing the optical rotation data of pyridoxatin, E. Lacey (Microbial Screening Technologies) for an authentic sample of tenuazonic acid, A. Blumenthal (UQ Diamantina Institute) and A. Jarrad (Institute for Molecular Bioscience) for additional bioassay support, and F. H. Song (Institute of Microbiology, Chinese Academy of Sciences) for advice on structure elucidation. Z. S. acknowledges the provision of an International Postgraduate Research Scholarship (IPRS) and a Centennial Scholarship by the University of Queensland. B. P. E. acknowledges a grant from São Paulo Research Foundation (FAPESP 13/13166-4). This research was funded in part by the Institute for Molecular Bioscience, the University of Queensland and the Australian Research Council (DP120100183, LP120100088).

Notes and references

1 X. Liu, F. Song, L. Ma, C. Chen, X. Xiao, B. Ren, X. Liu, H. Dai, A. M. Piggott, Y. Av-Gay, L. Zhang and R. J. Capon, *Tetrahedron Lett.* 2013, **54**, 6081.

- 2 F. Song, X. Liu, H. Guo, B. Ren, C. Chen, A. M. Piggott, K. Yu, H. Gao, Q. Wang, M. Liu, X. Liu, H. Dai, L. Zhang and R. J. Capon, *Org. Lett.* 2012, **14**, 4770.
- 3 L. J. Fremlin, A. M. Piggott, E. Lacey and R. J. Capon, *J. Nat. Prod.* 2009, **72**, 666.
- 4 R. J. Capon, C. Skene, M. Stewart, J. Ford, R. A. O'Hair, L. Williams, E. Lacey, J. H. Gill, K. Heiland and T. Friedel, *Org. Biomol. Chem.* 2003, **1**, 1856.
- 5 R. Ratnayake, L. J. Fremlin, E. Lacey, J. H. Gill and R. J. Capon, *J. Nat. Prod.* 2008, **71**, 403.
- 6 H. Mikula, E. Horkel, P. Hans, C. Hametner and J. Fröhlich, *J. Hazard. Mater.* 2013, **250–251**, 308.
- 7 Y. Ujihara, K. Nakayama, T. Sengoku, M. Takahashi and H. Yoda, *Org. Lett.* 2012, **14**, 5142.
- 8 S. Aoki, K. Higuchi, Y. Ye, R. Satari, and M. Kobayashi, *Tetrahedron*, 2000, **56**, 1833.
- 9 K. Schmidt, U. Riese, Z. Li and M. Hamburger, *J. Nat. Prod.* 2003, **66**, 378.
- 10 C. Kasetrathat, N. Ngamrojanavanich, S. Wiyakrutta, C. Mahidol, S. Ruchirawat and P. Kittakoop, *Phytochemistry*, 2008, **69**, 2621.
- 11 T. Nakada, M. Nakajima, H. Kobayashi, M. Takahashi and I. Tanaka, *Jpn. Kokai Tokkyo Koho*, Vol. JP 2007153840 A 20070621, 2007.
- 12 L. Du, A. J. Robles, J. B. King, D. R. Powell, A. N. Miller, S. L. Mooberry and R. H. Cichewicz, *Angew. Chem. Int. Ed. Engl.* 2014, **53**, 804.
- 13 D. Siegel, S. Merkel, W. Bremser, M. Koch and I. Nehls, *Anal. Bioanal. Chem.* 2010, **397**, 453.
- 14 A. R. Healy, F. Vinale, M. Lorito and N. J. Westwood, *Org. Lett.* 2015, **17**, 692.
- 15 A. A. Yakasai, J. Davison, Z. Wasil, L. M. Halo, C. P. Butts, C. M. Lazarus, A. M. Bailey, T. J. Simpson and R. J. Cox, *J. Am. Chem. Soc.* 2011, **133**, 10990.
- 16 H. V. Kemami Wangun and C. Hertweck, *Org. Biomol. Chem.* 2007, **5**, 1702.
- 17 R. W. Hooft, L. H. Straver and A. L. Spek, *J. Appl. Crystallogr.* 2008, **41**, 96.
- 18 Y. Teshima, K. Shin-ya, A. Shimazu, K. Furihata, H. S. Chul, K. Furihata, Y. Hayakawa, K. Nagai and H. Seto, *J. Antibiot.* 1991, **44**, 685.
- 19 L. M. Halo, M. N. Heneghan, A. A. Yakasai, Z. Song, K. Williams, A. M. Bailey, R. J. Cox, C. M. Lazarus and T. J. Simpson, *J. Am. Chem. Soc.* 2008, **130**, 17988.
- 20 A. Hölzel, M. G. Gänzle, G. J. Nicholson, W. P. Hammes and G. Jung, *Angew. Chem. Int. Ed. Engl.* 2000, **39**, 2766.
- 21 D. U. Ganihigama, S. Sureram, S. Sangher, P. Hongmanee, T. Aree, C. Mahidol, S. Ruchirawat and P. Kittakoop, *Eur. J. Med. Chem.* 2015, **89**, 1.
- 22 R. Kumar, R. Subramani, K. D. Feussner and W. Aalbersberg, *Mar. Drugs*, 2012, **10**, 200.
- 23 S. B. Singh, D. L. Zink, B. Heimbach, O. Genilloud, A. Teran, K. C. Silverman, R. B. Lingham, P. Felock and D. J. Hazuda, *Org. Lett.* 2002, **4**, 1123.
- 24 B. Biersack, R. Diestel, C. Jagusch, F. Sasse and R. Schobert, *J. Inorg. Biochem.* 2009, **103**, 72.

ARTICLE

Journal Name

- 25 A. Pansanit, E. J. Park, T. P. Kondratyuk, J. M. Pezzuto, K. Lirdprapamongkol and P. Kittakoop, *J. Nat. Prod.* 2013, **76**, 1824.
- 26 P. R. Graupner, A. Carr, E. Clancy, J. Gilbert, K. L. Bailey, J. A. Derby and B. C. Gerwick, *J. Nat. Prod.* 2003, **66**, 1558.
- 27 G. F. Kaufmann, R. Sartorio, S. H. Lee, C. J. Rogers, M. M. Meijler, J. A. Moss, B. Clapham, A. P. Brogan, T. J. Dickerson and K. D. Janda, *Proc. Natl. Acad. Sci.* 2005, **102**, 309.
- 28 H. J. Lee, M. C. Chung, C. H. Lee, H. K. Chun, H. M. Kim and Y. H. Kho, *J. Microbiol. Biotechnol.* 1996, **6**, 445.
- 29 J. P. Michael and G. Pattenden, *Angew. Chem., Int. Ed. Engl.* 1993, **32**, 1.
- 30 B. P. Espósito, S. Epsztejn, W. Breuer and Z. I. Cabantchik, *Anal. Biochem.* 2002, **304**, 1.
- 31 K. N. Raymond, G. Müller and B. F. Matzanke, *Top. Curr. Chem.* 1984, **123**, 49.
- 32 G. J. Kontoghiorghes, E. Eracleous, C. Economides and A. Kolnagou, *Curr. Med. Chem.* 2005, **12**, 2663.
- 33 G. M. Sheldrick, *Acta Crystallogr. A* 2008, **64**, 112.
- 34 L. J. Farrugia, *J. Appl. Crystallogr.* 1997, **30**, 565.
- 35 L. J. Farrugia, *J. Appl. Crystallogr.* 1999, **32**, 837.